조선대학교
CHOSUN UNIVERSITY

August 2021
Master's Degree Thesis

Green synthesis of silver Nanoparticles using Glycerol or In-Site Synthesis of Silver Nanopartcles inside Silver Citrate Nanorods

Graduate School of Chosun University

Department of Chemistry

Liu Tianhao

Green synthesis of silver Nanoparticles using Glycerol or In-Site Synthesis of Silver Nanopartcles inside Silver Citrate Nnnorods

글리세롤을 이용한 은 나노입자 녹색 합성 및 은-시트레이트 나노로드 내부에서의 현장합성

August 27, 2021

Graduate School of Chosun University

Department of Chemistry

Liu Tianhao

Green synthesis of silver Nanoparticles using Glycerol or In-Site Synthesis of Silver Nanopartcles inside Silver Citrate Nnnorods

Advisor: Prof. Lim Jong-Kuk

A thesis submitted in partial fulfillment of the requirements for a Master's degree

April 2021

Graduate School of Chosun University

Department of Chemistry

Liu Tianhao

Confirmation of Master's Thesis

위원장　조선대학교 교 수　손 홍 래 (인)

위　원　조선대학교 교 수　이 종 대 (인)

위　원　조선대학교 교 수　임 종 국 (인)

May, 2021

Graduate School of Chosun University

TABLE OF CONTENTS

LIST OF FIGURES

ABSTRACT

Green Snthesis of Silver Nanoparticles Glycerol or In-Site
Synthesis of Silver Nanoparticles inside Silver

Tianhao Liu

Advisor: Prof. Lim Jong-kuk, Ph.D.

Department of Chemistry

Graduate School of Chosun University

Glycerol is a substance with good economy. Researchers have been looking
forward how to make it valuable. A new scheme is to use glycerol as a
"green solvent" to instead of petroleum-based organic solvents. Its nonhazardous
to human body, and high boiling point allow to perform experiment at high
temperatures under ambient atmospheric pressures. Its dielectric constant is
between that of water and organic solvents, and it can dissolve a variety of
substances between salts and organic molecules. A lot of report shows that metal
nanoparticles could be synthesized in glycerol, but it often has high requirements
on the conditions, such as high temperatures, alkaline pH conditions or irradiance
of ultraviolet light. Herein, we prove that silver nanoparticles could be reduced
in glycerol under a condition without external energy intervention. We found it
was based on aldehydes and free radicals which were generated in glycerol. They
would be acting as reducing agent in operation. And silver nanoparticles often be
used as antimicrobial agents, but an important risk factors is that could be damage
human body also, when it is used as a topical medicine. An idea to solve this
problem is to embed the nanoparticles in matrices such as composites, polymers

or hydrogels. However, most methods have limitations in terms of nanoparticles loading capacity or pre- or post-treatment require in the manufacturing process. Herein, we report that two in-situ synthetic of silver nanoparticles inside silver citrate nanorods that rea antimicrobial composed of silver and citrate ions. The advantage of silver nanoparticles embedded silver citrate nanorods are exhibit a synergistic, long-lasting, and sustainable antimicrobial effect. And it's worth noting that the nanoparticles can be formed inside silver citrate nanorods rapidly via electron beam irradiation without high temperature or add other reagents. The funda-mental principles of the proposed efficient syntheses are discussed in terms of the catalytic effect of reactants condined in nanospaces.

한글요약

고신뢰 FPGA를 위한 동의 보팅 기법

유천호

지도 교수: 임종국

화학과

대학원, 조선대학교

은 나노 입자는 다양한 분야에서 사용될 수있다. 항균, 광전자 공학 및 표면 강화 라만 산란 (SERS) 감지 등. 대부분의 문헌에 따르면은 나노 입자는 고온, 알칼리성 pH 조건 및 자외선 조사에 의해 합성됩니다. 그리고 우리는 green 경로를 통해은 나노 입자를 합성하는 방법을 소개한다. 이 방법은은 이온과 반응하여은 나노 입자를 합성하는 환원제 인 글리세롤을 사용했다. 이 방법의 장점은 완전히 green 조건에서 모든 반응이 가능하다는 것인다. 이는 실온, 중성 pH 조건 및 에너지 원이 없음을 의미한다. 그리고 나서 은이나 은 이온 소금 나노 입자의 응용에 초점을 맞춘다. 우리는 항균제로 만들기 위해 일종의 은 구연산 나노입자를 합성한다. 은색 나노입자가 들어 있는 은색 구연산 나노로드인다. 그 부피 때문에, 은구연산 나노로드들은 신체에 손상을 주지 않고 은 나노입자를 천천히 방출하는 피부 표면에서만 활동할 수은하 나노입자를 방출할 수 있었다.

I.   INTRODUCTION

1.   synthesis metal nanoparticles with glycerol

At beginning of 21st century, using glycerol to synthesis copper nanoprticles be reported. In that case, the copper salt and glycerol reaction under atmospheric conditions at above 200°C, close the boiling point of glycerol. and silver nanoparticles be formed by glycerol at 175°C in 2004. And in 2010, it's first to synthesis silver nanoparticles by glycerol at room temperature under alkaline condition. Reduction of metal ions in glycerol is usually explained by three mechanisms: catalytic reduction, aldehyde reduction, or alkyd reduction.Under alkaline conditions, silver ions readily interact with hydroxide ions to form silver oxide particles.The surface of preformed silver oxide particles in alkaline solution at room temperature can catalyze the reduction of silver ions.Metallic ions are known to be reduced by aldehydes, such as the "Tollens reaction", which can be formed by dehydration of glycerol or alkaline glycerol during heating.Another mechanism is the hydroxide ion reducing alcohol salts, alcohols or aldehydes or ketones.According to this mechanism, the conversion of glycerol to aldehydes is not necessary because the alcohol salts can directly reduce metal ions.These three mechanisms provide a reasonable explanation for the synthesis of metal nanoparticles in glycerol, but some of the experimental results shown here cannot be explained.For example, all of the above mechanisms emphasize alkaline conditions because hydroxide ions are essential for the synthesis of metal nanoparticles.However, experiments have shown that there is no need for alkaline conditions and that silver nanoparticles can be synthesized even under neutral conditions.

2.   silver nanoparticle-embedded antimicrobial materials

Many researchers fabricating silver nanoparticle-embedded materials for make anti-oxidation and microbial nanoparticles can penetrate and prevent release into liquids or tissues. These methods consist of 1) adsorbing the previously synthesized silver nanoparticles on the substrate, 2) reducing the pre-adsorbed silver ions through an external reducing agent, and 3) adsorbing and reducing silver ions after reduction to the substrate. In the first method, silver nanoparticles are made and then adsorbed onto a substrate (shell sorbent film or modified glass surface). Since the silver nanoparticles are relatively large and do not effectively penetrate into these matrices, their use in a three-dimensional matrix is difficult. The second method is to reduce the silver ions inside the substrate by adsorbing the silver ions onto the substrate containing the chemically active group that binds the silver ions, and then adding a reducing agent to reduce the silver ions inside the substrate. Silver nanoparticles are adsorbed and dispersed well inside the substrate. However, in this method, silver ions must be reduced by adding a reducing agent to the substrate. In the third method, a functional group capable of restoring silver ions is first drawn into the substrate, and then a functional group capable of restoring silver ions is attracted to the substrate. The substrate was made to adsorb silver ions. The silver ions were reduced to silver nanoparticles inside the substrate without the addition of a reducing agent. This method requires an additional procedure for pre-functionalization of the substrate without adding a reducing agent.

II. Green Synthesis of Silver Nanoparticles with Homogeneous Size Distribution in Glycerol at Neutral pH and Ambient Temperature

1. Introduction

Recently, with increase of biodiesel demand over the world, the production of glycerol, which is byproduct of biodiesel, has also increased for the past decade[1] . Because biodiesel has more advantages than conventional fossil fuels in the viewpoint of environment and energy efficiency, biodiesel production is expected to continuously grow in the future[2], [3] , and lead to a larger surplus of glycerol with a subsequent reduction of its market price[4], [5] . Many scientists and engineers have been concerned about the economical ways of mass consumption for oversupplied glycerol, and tried to find new chemistry of glycerol in various applications such as conversion into valuable chemicals (ethylene glycol, ethanol, or citric acid etc.)[4], [6], hydrogen gas production, or additives for a variety of products (cosmetics, foods, or pharmaceuticals etc.) . In 2007, Wolfson's group added one more application of glycerol for its mass consumption, and that was the use of glycerol as a "green solvent"[7] . Since the movement of "green chemistry" started in the late 1990s', searching for environmental benign, replaceable for petroleum-based organic solvents, so called "green solvent", has been one of the major issues in the community of green chemistry[8] . Because glycerol is not only non-toxic, renewable, and biodegradable, but also able to dissolve wide range of compounds spanning from inorganic salts, acids, and bases to organic compounds that are poorly soluble in water, it can be a good candidate for green solvent. In addition to this,

because glycerol has high boiling point and low vapor pressure, chemical reaction can be performed in a glycerol solvent at high temperature under atmospheric pressure for a long period. The first chemical reaction in a glycerol solvent was demonstrated by Wolfson's group, in which they showed that several catalytic and non-catalytic reactions could be successfully performed in a glycerol solvent. Since then subsequent wide variety of chemical reactions have been successfully developed by other groups[9], [10] . On the same line, the synthesis of metal nanoparticles in a glycerol solvent began to receive attention again as a green pathway. Amit Shinha et al. published the first report concerning the synthesis of metal particles in a glycerol solvent in 2002, several years before the emergence of glycerol as a green solvent[11] . In that paper, authors synthesized micron-sized copper particles in glycerol at near boiling point of glycerol (230°C). After first demonstration in 2002, other metal particles (gold, silver, and platinum etc.) were also synthesized in the same medium at high temperature of over 100°C[12]–[16] . In these reactions, glycerol is generally known to serve as both a solvent and a reducing agent. Although there are few papers describing a detailed mechanism of how glycerol reduces metal ions at high temperature, resulting in the formation of metal particles, it is believed that the reduction process is carried out by the aldehyde (e.g., glyceraldehyde) converted from alcohol (e.g., glycerol) at high temperature when referring to the previous papers[17]–[20] . The reduction process of metal ions by glycerol is possible not only at high temperature but also at room temperature. In 2010, Adjana Sarkar et al. found that silver nanoparticles could be synthesized in a glycerol solvent even at room temperature without adding any reducing agents, when sodium hydroxide (NaOH) was added[21] . In this paper, based on the knowledge learned from previous research papers, authors suggested a plausible mechanism for

4

the reduction of silver ions and subsequent formation of silver nanoparticles at room temperature under highly alkaline condition, but did not show any direct evidences. To date, many research papers on the synthesis of metal nanoparticles in glycerol has been reported, and most of reactions were performed at high temperature or under alkaline condition[22]–[28] . The reduction of metal ions in glycerol is generally explained by three mechanisms: catalytic reduction[21], [29] , reduction by aldehydes[18], [21] , or reduction by alkoxides[28] . Under alkaline condition, silver ions easily interact with hydroxide ions and form silver oxide (Ag_2O) particles[30] . Silver ions could be catalytically reduced on the surface of silver oxide particles pre-formed in alkaline solution at room temperature[29] . It has already been known for metal ions to be reduced by aldehydes such as "Tollens reaction", and aldehyde could be formed through dehydration process of glycerol in heated or alkaline glycerol[19], [20] . Another mechanism is the reduction by alkoxides that could be formed from alcohols, aldehydes, or ketones by hydroxide ions. According to this mechanism, glycerol does not need to be converted to aldehydes, because alkoxides generated from alcohols can reduce metal ions directly[28] . These three mechanisms provide reasonable explanations for the synthesis of metal nanoparticles in glycerol, but some experimental results we will show herein cannot be explained by these mechanisms. For example, all mechanisms suggested above emphasize alkaline condition due to hydroxide ions that are essential for the synthesis of metal nanoparticles. According to our experiments, however, alkaline condition is not essential, and silver nanoparticles can be synthesized in glycerol even in neutral condition. In this report, we propose novel mechanism for the synthesis of silver nanoparticles in glycerol and discuss it with direct evidences.

2.　　Experimental

2.　1.　　Chemicals and apparatuses

Silver nitrate ($AgNO_3$, 99.0%, Aldrich), glycerol ($C_3H_8O_3$, 99.0%, Daejung), polyvinylpyrrolidone (Ave. M.W. 40,000, Aldrich) were used without further purification, and highly purified deionized (DI) water (18.2 Mcm) produced using QPAK1 (MILLI Pore) was used for all aqueous solutions to prepare silver nanoparticles. For detecting aldehydes and free radicals in a glycerol, Schiff's reagent for aldehydes (Sigma) and 2,2-diphenyl-1-picrylhydrazyl (DPPH) (95%, Alfa Aesar) were purchased and used as received. All apparatuses were treated with "piranha" solution (acidic solution mixed with concentrated sulfuric acid (H_2SO_4) and 40% of hydrogen peroxide (H_2O_2) by 4 to 1 ratio (v/v)) for at least 2 hours and dried in oven at $70^\circ C$ until completely dry.

2.　2.　　Preparation of silver nanoparticles in glycerol

To synthesize silver nanoparticles in a glycerol, usually, silver nitrate was not dissolved directly into a glycerol, due to its slow dissolution rate in a glycerol solvent. Instead, silver nitrate solution was firstly prepared in DI water, and then mixed it up with a glycerol solvent. More specifically, silver nitrate (85 mg) was firstly dissolved into a small amount of water (0.1 mL) instead of glycerol (Scheme 1(a, b)), and then 0.1 mL silver nitrate aqueous solution was added to 4.9 mL of glycerol (Scheme 1(c) and (d)). The finally obtained mixed solution was transparent as shown in the picture ((a)-1) of the Scheme 1(d). If this solution was placed on a shelf of laboratory at room temperature (20   25C) for a few tens of hours, the color of the solution turns into a color visible to the eye, meaning the formation of silver nanoparticles. To prepare stabilized silver nanoparticles, DI

6

water and glycerol containing PVP (40%, w/v, respectively) was used instead of pure solvents. The PVP was quickly dissolved into water; however, it took several days for PVP to be completely dissolved into glycerol at room temperature.

2.   3.   **Characterizationl**

The formation of silver nanoparticles was confirmed by observing the color of the solutions and their UV-Vis spectra obtained by spectrophotometer (UH5300; Hitachi). The size distribution of nanoparticles was obtained by measuring their diameters in electron micrographs taken by scanning electron microscope (FE-SEM, S-4800; Hitachi) or transmission electron microscope (TEM, JEM-3010; JEOL). Infrared (IR) spectroscopy and colorimetric method were used for detecting aldehydes in a glycerol. IR spectra were obtained for glycerol using IR spectrometer (6700; Thermo Fisher Scientific) in attenuated total reflection (ATR) mode on a zinc selenide with 200 accumulations. In colorimetric method, Schiff's reagent (1 mL), which is transparent solution but its color changes into violet in the presence of aldehydes, was mixed with 2 mL of glycerol and its color change was monitored. The presence of free radicals in a glycerol was also investigated using colorimetric reagents, 2,2-diphenyl-1-picrylhydrazyl (DPPH) (95%, Alfa Aesar), which is violet powder in ambient conditions. Because DPPH was slowly dissolved in glycerol, ethanolic solutions of DPPH (0.1 mM) were firstly prepared, and they are added into the glycerol tested by 1 to 1 ratio (v/v). The color of the solution is changed from violet into yellow under the presence of free ridicals.

Scheme 1. The scheme of synthesis of silver nanoparticles with silver nitrate and glycerol under nature condition.

3.   Results and discussion

Most of the papers published to date deal with the synthesis of metal nanoparticles in a glycerol solvent only at high temperature or in alkaline condition. Therefore, the synthetic mechanism has been focused on the role of heating or hydroxide ions for structural change of glycerol into molecules that can act as reducing agents. Recently, we found that silver nanoparticles are formed in a glycerol solvent even at room temperature (20 25°C) and in neutral pH condition without any extra additives. Figure 1 is a representative case of our findings, in which about 85 mg of silver nitrate is dissolved into a small amount of water (0.1 mL) (Scheme 1(a, b)), and then 0.1 mL of silver nitrate aqueous solution was added to 4.9 mL of glycerol solvent (Scheme 1(c, d)). The color of the solution is initially transparent ((a)-1 in Scheme 1(d) and in

Figure 1(a)), however, begins to change into orange color ((a)-2 in Figure 1(a) and black solid line in Figure 1(b)), after several hours. This orange color and spectral profile showing the maximum near 400 nm is traditional characteristics of spherical silver nanoparticles with several tens of nanometers in diameter. In this case, because extra additives, such as sodium hydroxide, even any stabilizers was not added, and reaction was performed at room temperature, it can be said with certainty that silver nanoparticles are synthesized in a glycerol solvent by mechanism different from those generally accepted. As the reaction time gets longer, the color of the solution gradually changes. After about 27 hours, the color of the solution changes to greyish orange ((a)-3 in Figure 1(a)) concomitant with spectral broadening in red line of Figure 1(b). And at last, the orange color is disappeared and the color of the solution turns grey after about 46 hours ((a)-4 in Figure 1(a)) and their spectral width becomes more broad (blue line in Figure 2(c)), which means that nanoparticles grow inhomogeneously and glycerol solution contains silver nanoparticles of various sizes. This is more clearly confirmed in electron micrograph (Figure 2(a)) and its energy dispersive spectrum (Figure 2(b)), which shows that although the sizes of nanoparticles are various (average diameter 38 13 nm), silver nanoparticles are certainly formed in a glycerol solvent without any extra additives. In this experiment, a little amount of water does not affect to nanoparticle formation. As demonstrated as black line in Supporting Figure 1, silver nanoparticles are also synthesized in pure glycerol solvent without adding water. In this case, however, dissolution rate of silver nitrate is very slow. It takes about a few hundred hours to fully dissolve 85 mg of silver nitrate in 5 mL of glycerol completely. Due to slow dissolution of silver nitrate in glycerol, the concentration of silver ions in glycerol is slowly increased, and seeds are also slowly produced. According to the nucleation theory on the

synthesis of nanoparticles, it is expected that the slow rate of seed formation leads to the broad size distribution of nanoparticles, and this expectation is observed in the broad spectrum represented as blue line in Supporting Figure 1(a), and scanning electron micrograph in Supporting Figure 1(b).
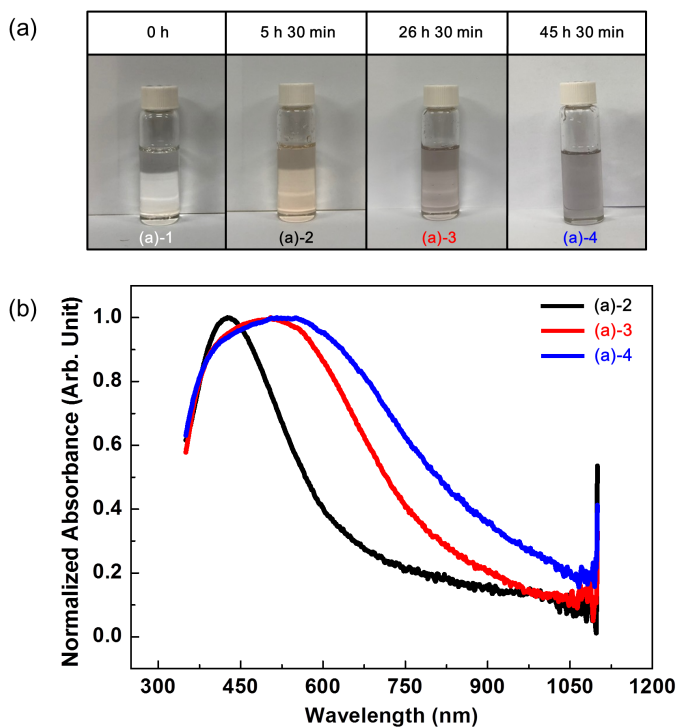
Figure 1: Chronological sample photos, (a) and corresponding UV-Vis spectra, (b). The color of the glycerol solution containing silver ions gradually changed to light orange and finally to grey. Concomitant with these color changes, the width of spectra becomes broaden.

11
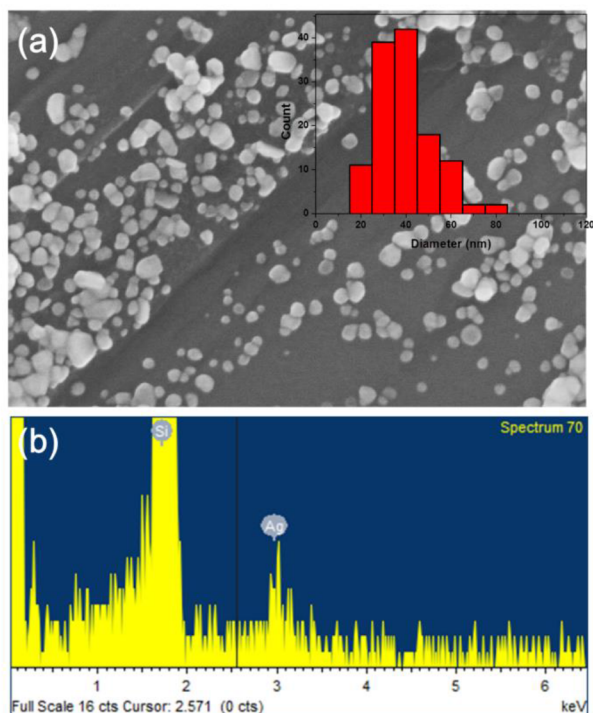
Figure 2: Electron micrograph, (a) and its energy dispersive spectrum, (b) of silver nanoparticles prepared in glycerol without stabilizer, polyvinyl pyrrolidone..

So far, we discussed about the synthesis of silver nanoparticles in a glycerol solvent. In this reaction, glycerol must play an important role as reducing agents at room temperature in neutral pH condition. If this is true, what is the mechanism for this reaction? How does glycerol reduce silver ions at room temperature and in neutral pH condition? We can obtain some clues for the reduction mechanism of glycerol suggested in previous paper [16], which states that ethylene glycol

12

can be converted to glycoaldehyde by oxygen (Chemical Equation (1)) and the converted glycoaldehyde reduce the silver ions. We think that the similar conversion and reduction can occur in a glycerol solvent (Chemical Equation (2)). Similar to the case of ethylene glycol, glycerol may also be converted to glyceraldehyde, and silver ions may be reduced by the converted glyceraldehyde. To verify that this mechanism is correct, we tried infrared spectroscopy.

$$2 \; HO{-}\!\!\diagdown\!\!{-}OH + O_2 \longrightarrow 2 \; O{=}\!\!\diagup\!\!{-}OH + 2H_2O \qquad \text{(Equation 1)}$$

$$2 \; \overset{OH}{\diagup}\!\!{-}OH + O_2 \longrightarrow 2 \; \overset{O}{\diagup}\!\!{-}OH + 2H_2O \qquad \text{(Equation 2)}$$
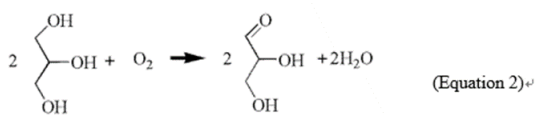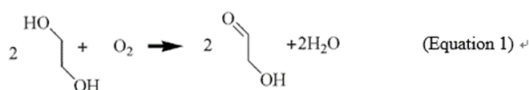
According to the chemical equation (2), the concentration of glyceraldehyde is proportional to the amount of dissolved oxygen. In order to confirm the presence of glyceraldehyde generated by oxygen in glycerol, we prepared a total of three types of glycerol, manufactured in different years and prepared in different ways. Old and new glycerol manufactured last and this year, respectively (based on the vendor-provided specification), were used without any treatment, and another glycerol was prepared by purging new glycerol (manufactured this year) with air for about two weeks. Since the old glycerol, and the new glycerol

13
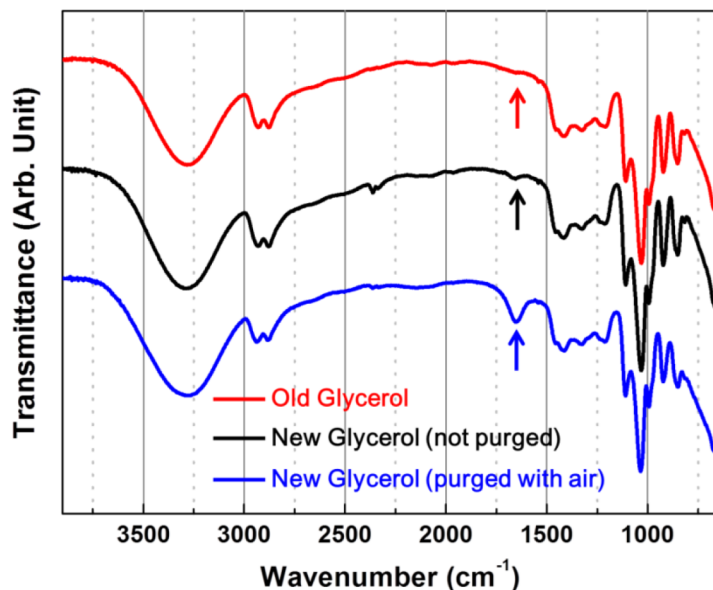
Figure 3: The IR spectra of 3 kinds of glycerols (old glycerol produced last year, new glycerol produced this year and new glycerol purged with air for about two weeks.

purged with air would have had more opportunities to be exposed to oxygen in the air, the amount of dissolved oxygen concomitant with the concentration of glyceraldehyde could be higher than that in the untreated new glycerol. IR spectra for three samples were obtained using attenuated total reflection (ATR) method, and their spectra were compared with together as shown in Figure 3. Three spectra do not show characteristic peaks of

carbonyl group at around 1730 cm-1, and are almost identical except for the band that appears at 1650 cm-1 as represented with arrows in Figure 3. A closer look at around 1650 cm-1 of the three spectra reveals that this peak appears not only in purged new glycerol (blue line in Figure 3) but also in other glycerols (black and red lines in Figure 3), although their strength is different in each spectrum. The IR band appeared at near 1650 cm-1 can be attributed to the hydrogen-bonded carbonyl stretching mode. Generally, the stretching mode of carbonyl groups in aldehyde appears at 1720   1740 cm-1. However, if the bond strength of C=O becomes weak through the loss of double bond character by hydrogen bond, or hybridization, the vibrational frequency can be shifted to lower energy region, resulting in appearance of carbonyl band at   1650 cm-1. Because, in general, glyceraldehyde can form intra hydrogen bonding followed by dimeric hemiacetal [31], [32], it is possible that stretching band of C=O appears at   1650 cm-1. Because the concentration of glyceraldehyde, however, should be low not enough to form dimer, and the portion of dimer would not be high, this assignment could be excluded. This peak could also arise from O-H scissoring of water molecules contained in glycerol because glycerol is so hygroscopic that glycerol can effectively absorb water molecules from the atmosphere to some extent [33]. Since the amount of water contained in glycerol equilibrates with the humidity of atmosphere, the intensity of the peak appearing at around 1650 cm-1 in each spectrum should be variable according to atmospheric condition. Nevertheless, the intensity of the near 1650 cm-1 in blue line (the new glycerol purged with air) is exceptionally strong compared to other two spectra, probably because a large amount of water was produced and contained in the new glycerol purged with air by the chemical equation (2). Since the amount of water in glycerol can be estimated from its density [34], we measured the density of three

15

glycerols and compared the amount of water contained in glycerol as weight-to-weight percent. As a result, we found that the glycerol purged with air contained extraordinarily larger amount of water (19%, w/w) 19 times more than that in other two glycerols (both 1%, w/w). The strong IR peak appearing at 1650 cm-1 and high water concentration in the purged new glycerol state that glycerol reacts with dissolved oxygen and produced glyceraldehyde and water as described in chemical equation (2). From the density measurement, we also found that the amount of water content in the purged new glycerol was not maintained and became decrease, as time goes by. This is probably because the concentration of water in glycerol equilibrates with atmospheric water concentration. And this equilibrium of water concentration in between glycerol and atmosphere would be also reason why the peak intensity at around 1650 cm-1 of old and new glycerol is similar value. Although many glyceraldehyde and water were produced in old glycerol, the water concentration of old glycerol could be similar with that of new glycerol, due to equilibration of water.

Glyceraldehyde in glycerol might be detectable in a more sensitive technique. Of the various analytical methods, traditional colorimetric methods are so simple and sensitive as much as IR spectroscopy that we adopted colorimetric method, especially "Schiff method" to reconfirm the presence of glyceraldehyde in glycerol. In this method, specially designed molecule, fuchsin-sulfite reagent named as "Schiff reagent" is mixed with the analyzed target solution and the presence of aldehyde is determined by the appearance of magenta color in the mixed solution. In order to investigate the presence of aldehydes produced by dissolved oxygens in glycerol, 1 mL of Schiff solution was mixed with 2 mL of old and new glycerol at room temperature (20   23°C) with allowance of ambient light. The color of the mixed solution was investigated after required

16

(a)

Type	Old	New	New	New	New
Temperature	RT	RT	RT	RT	RT
Ambient Light	O	O	O	O	O
Purging	✕	✕	✕	O	O
Waiting Time	15 min	15 min	1 hr	15 min	1 hr
Result of Schiff's Test	4(a)-1	4(a)-2	4(a)-3	4(a)-4	4(a)-5

(b)
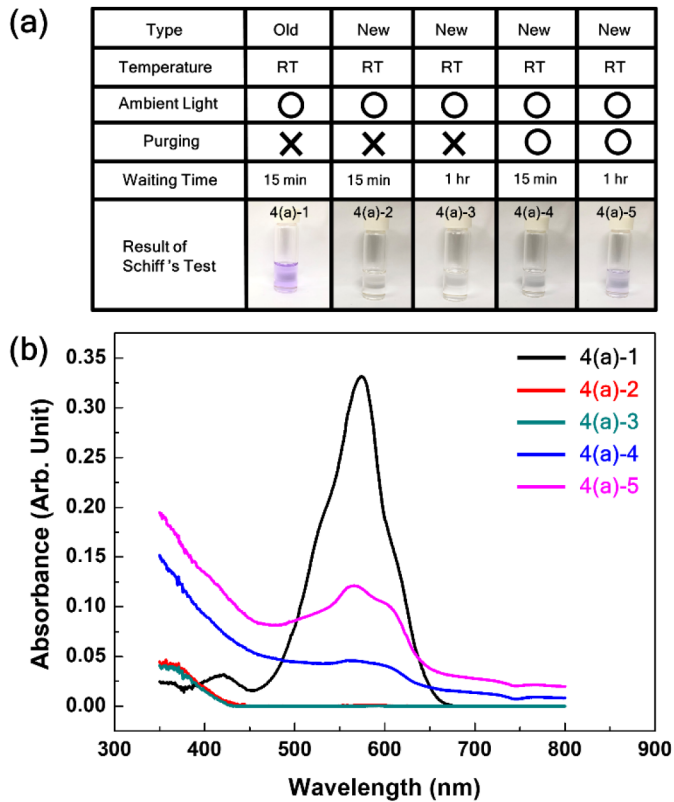
Figure 4: The Schiff's test result of various kinds of glycerols, (a) and their UV-Vis spectra, (b). Violet color means that aldehydes are contained in test solution. Only old glycerol manufactured in last year (4(a)-1) shows violet color. And the color of new glycerol manufactured in this year is colorless and transparent but if it is purged with air, their colors change to violet.

periods (15 min or 1 hr). The picture 4(a)-1 and 4(a)-2 of Figure 4(a) were taken 15 minutes after mixing glycerol and Schiff reagent. Interestingly, the color of the glycerol was changed into magenta only in old glycerol, but the color of the new glycerol was not changed, which means that aldehyde exists in only old glycerol and not in new glycerol. Although waiting time is prolonged to 1 hour, the color change is not observed (4(a)-3 in Figure 4(a)) in new glycerol. The color change can be observed more sensitively using UV-Vis spectrophotometer (Figure 4(b)). Contrary to the strong absorbance in black solid line which is the absorption spectrum corresponding to 4(a)-1 in Figure 4(a), absorption spectra of 4(a)-2, and even 4(a)-3 do not show any absorbance at wavelengths above 450 nm as represented as red and green solid line in Figure 4(b). Under these experimental results, it is well predicted that some glycerol could be converted to glyceraldehyde by oxygen dissolved in old glycerol, while such conversion rarely occurs in a new glycerol due to low amount of dissolved oxygen. To further confirm the oxygen effect, new glycerol was purged with air using bubble stone for about 40 hours, and Schiff test was conducted again. Because purging with air increases the amount of dissolved oxygen, resulting in generation of glyceraldehyde in a new glycerol, it is expected that aldehyde can be possibly detected, that is, magenta color appears in the new glycerol purged with air. As expected, the color of the new glycerol purged with air was changed into magenta as shown in 4(a)-4 of Figure 4(a), which is taken 15 minutes after mixing. Although the magenta color is not clear in the picture 4(a)-4, but in the UV-Vis spectrum, absorption peak distinctively appeared at wavelengths between 450 and 650 nm (blue solid line in Figure 4(b)) in the UV-Vis spectrum. In addition, when the waiting time is prolonged until 1 hour after mixing, the color of the solution becomes more clear (4(a)-5 of Figure 4(a)) concomitant

18

with increase of absorption peak (magenta solid line in Figure 4(b)). To the best of our knowledge, this is the first evidence revealed that glyceraldehydes are produced from glycerol by dissolved oxygen. The experimental results conducted above state that the old glycerol contains glyceraldehyde converted from glycerol by dissolved oxygen, but the newly produced glycerol does not contain glyceraldehyde. If glyceraldehyde is the only species that contribute to the formation of silver nanoparticles by reducing silver ions, nanoparticles are produced only in old

glycerol, but not in new glycerol. In reality, however, silver nanoparticles are synthesized in both old and new glycerol, which means that silver ions are reduced by not only glyceraldehyde but also other species. Referring to the previous papers related to the synthesis of metal nanoparticles in glycerol [36, 37], we thought that some sort of free radicals would be produced and might affect nanoparticle synthesis. In order to investigate the formation of free radicals in glycerol, we adopted colorimetric method, in which relatively stable radical molecules (usually a certain color) are added as indicators into the glycerol. If there are free radicals formed in glycerol, they react with the indicators (radical molecules) followed by structural change of indicators, and finally resulting in color change. Herein, 2,2-diphenyl-1-picrylhydrazyl (DPPH) which is a violet solid compound at ambient condition was used as indicators. DPPH dissolves in glycerol but its dissolution rate is very slow. It takes about 20 hours with vigorous stirring to prepare 0.1 mM DPPH solution in glycerol. Therefore, DPPH firstly dissolved in ethanol to a concentration of 0.1 mM and the ethanolic solution containing DPPH was mixed with old and new glycerols in a 1:1 ratio (v/v), respectively. At the beginning, the color of the solution was violet as shown in the picture (5(a)-1 and 5(a)-4 in Figure 5(a)) regardless of the manufactured date

Type	Old	Old	Old	New	New	New
Temperature	RT	RT	RT	RT	RT	RT
Ambient Light	O	O	O	O	O	O
Purging	X	X	X	X	X	X
Waiting Time	0 min	30 min	15 hrs	0 min	30 min	15 hrs
Result of Radical Test	5(a)-1	5(a)-2	5(a)-3	5(a)-4	5(a)-5	5(a)-6
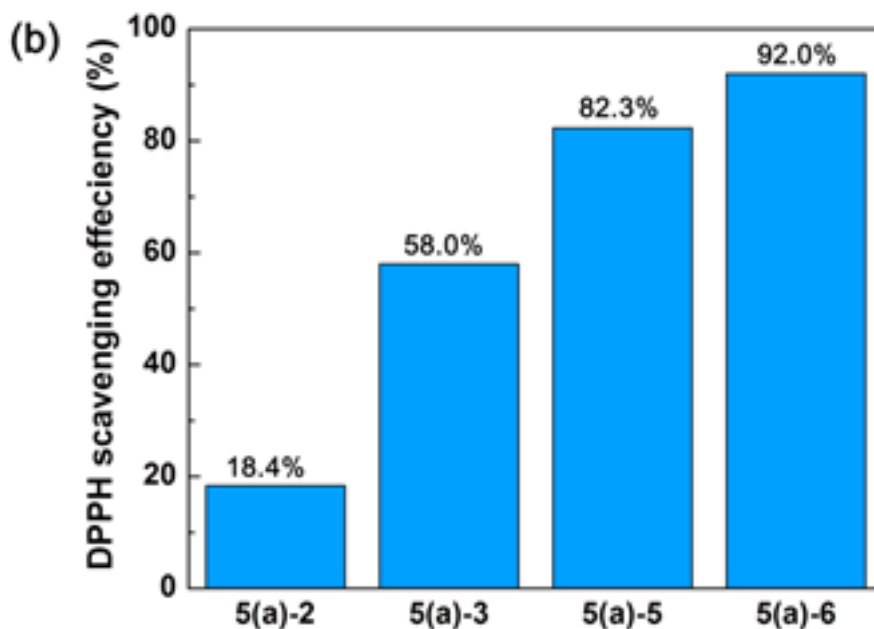
Figure 5: DPPH test result of old and new glycerols produced in last and this year, respectively at room temperature and under ambient light. In this test, when the solution contains radicals, the color of the solution changes from violet to yellow and "DPPH scavenging efficiency" is increased.

of glycerol. The mixed solutions were placed on the laboratory bench during required time (30 min or 15 hours) for the free radicals to be scavenged by indicators at room temperature (20°C) without protecting ambient light. The color of the mixed solutions was investigated after 30 min (5(a)-2 and 5(a)-5) and 15 hours (5(a)-3 and 5(a)-6). As compared to the initial color of the solution (5(a)-1 and 5(a)-4), the color of the old glycerol solution is hardly changed and still violet (5(a)-2 and 5(a)-3). The color of the new glycerol solution, however, has already begun to change into pink rose (5(a)-5)) after 30 min, and turned to yellow (5(a)-6) after 15 hours. It should be noted that ethanol did not affect to the scavenging efficiency as represented in Supporting Figure 2, in which the color of the ethanol was still violet even after 15 hrs. For quantitative analysis, UV-Vis spectra were taken (Supporting Figure 3) and scavenging efficiency was calculated for each sample using the equation(3).

DPPH scavenging efficiency $(\%) = (A_0 - A_1)/A_0 \times 100$ $\quad (equation 3)$

, where A_0, or A_1 is the area in between 500 and 550 nm in the UV-Vis absorption spectrum of the mixed solution (5(a)-1 or 5(a)-4) at the beginning stage or final stage after waiting for required time (5(a)-2, 3 and 5(a)-5, 6) after addition of DPPH, respectively. As represented in Figure 5(b), scavenging efficiency of new glycerol (82.3% for 30 min and 92.0% for 15 hrs) is higher than that of old glycerol (18.4% for 30 min and 58.0% for 15 hrs) by 4.5 times in 30 min, and 1.6 times in 15 hrs. This experimental result means that the concentration of free radicals in old glycerol is lower than that in new glycerol. Interestingly, this result shows the opposite trend from that of Schiff's test. That is, old glycerol with a high concentration of aldehydes contains low concentration of radicals and new glycerol with a low concentration of aldehydes contains high

21

concentration of radicals. To reconfirm these experimental results, we repeated the same experiment with various glycerols manufactured on different date, and found that all the tested glycerols shows the same trend (Supporting Figure 4). We think that free radicals are generated in both old and new glycerols, but glyceraldehydes present in old glycerols could play a role as a radical scavenger. Referring to the reference 37 in which glyceraldehyde radicals form dimer product, we can suggest the following chemical reaction (Equation 4) for the scavenging effect of glyceraldehydes, where free radicals snatch hydrogen radicals from glyceraldehydes and two glyceraldehydes radicals form dimer.
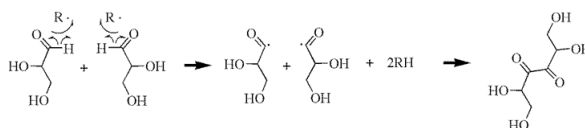
Scheme 2. The schematic chemical reaction representing scavenging effect of glyceraldehyde.

What is the energy source for generating free radicals in glycerol, especially in new glycerol? As the first candidate, we can suspect the ultraviolet or visible light mixed in the ambient light. Because we do not cover the vial containing glycerol, the glycerol is exposed to visible light and also have the chance to be exposed to even ultraviolet light. To confirm the light effect, we did DPPH

test for the same glycerol under different conditions, where one is placed right under LED light (6(a)-2), and the other one is covered with aluminum foil to block ambient light (6(a)-3). The temperature of the two glycerols was adjusted to 25°C and stabilized in the water bath for 15 hrs. The scavenging efficiency of the glycerol irradiated by LED light (6(a)-2) or the glycerol (6(a)-3) protected from ambient light is 79.3% or 71.4%, respectively. As shown in this value, light affects to DPPH scavenging efficiency but the effect is not so strong. It means that light irradiance is not main driving force for generating free radicals in glycerols. Another candidate for generation of free radicals in glycerol is temperature. When the same experiment was performed at -22°C, the scavenging efficiency sharply drops to 58.0% for the glycerol irradiated by LED light or to 49.2% for the non-irradiated glycerols. From this result, it can be concluded that the scavenging efficiency of DPPH is largely dependent on temperature more than light irradiance.

Based on the experimental results so far, glycerol can be divided into two types depending on what chemical species it contains. Since the glycerols newly produced do not have much chance to be exposed to oxygen, they contain small amount of aldehydes and relatively much amount of free radicals. Contrary to this, old glycerols would have had more chances to come in contact with oxygen and contain large amount of aldehydes and relatively small amount of free radicals. Because both glyceraldehydes and free radicals have reducing power, silver ions will be reduced mainly by glyceraldehyde in old glycerol, and reduced mainly by free radicals in new glycerols. These different pathways for the synthesis of silver nanoparticles in old and new glycerols could lead to different morphological properties (e.g., particle size and its size distribution) of the synthesized silver nanoparticles. Figure 7 is UV-Vis spectra and scanning electron

23

(a)

Type	New	New	New	New	New	New
Temperature	25°C	25°C	25°C	-22°C	-22°C	-22°C
LED Light	—	O	X	—	O	X
Purging	X	X	X	X	X	X
Waiting Time	0 min	15 hrs	15 hrs	0 min	15 hrs	15 hrs
Result of Radical Test	6(a)-1	6(a)-2	6(a)-3	6(a)-4	6(a)-5	6(a)-6

(b)
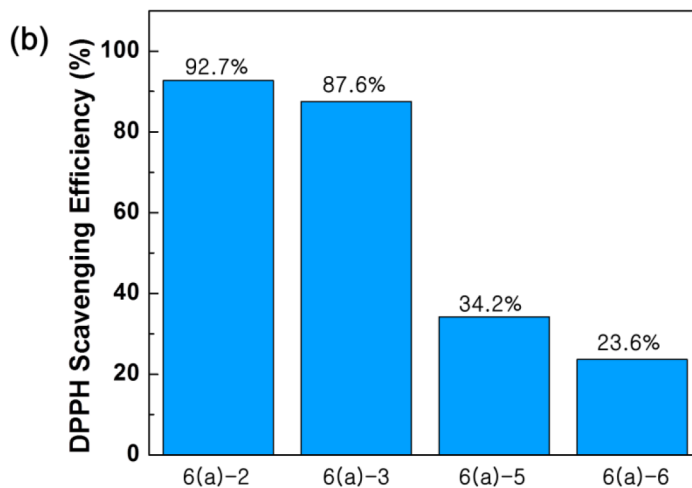
Figure 6: DPPH test result of new glycerol to investigate temperature and light effect for the generation of radicals.

micrographs for the silver nanoparticles produced in old and new glycerols. In this experiment, poly(vinyl pyrrolidone) was added to avoid the aggregation

24

effect of nanoparticles. Interestingly, as shown in Figure 7, the morphology of silver nanoparticles synthesized in old (Figure 7(b)) and new (Figure 7(c)) glycerols are much different. When the silver nanoparticles are synthesized in new glycerol, the color of the solution is yellow (left picture in the inset of Figure 7(b)), which is a representative color of the spherical silver nanoparticles with about 20 nm in diameter. This is also confirmed in its UV-Vis spectrum (black solid line in Figure 7(a)) and scanning electron micrograph (Figure 7(b)). When the silver nanoparticles are produced in old glycerols, the color of the solution is grey (the right picture in the inset of Figure 7(c)), which is quite different with the yellow solution in the inset of Figure 7(b). Usually, grey color represent the particle size is large and inhomogeneous, and this is well reflected on the broad UV-Vis spectrum (blue line in Figure 7(a)) and scanning electron micrograph of Figure 7(c) in which the particle size is ??? nm. What causes the different sizes and uniformities of nanoparticles in different types of glycerols? More research is needed on this, but we can find some explanation in the nucleation and growth theory of nanoparticles. According to nucleation and growth theory of nanoparticles, the period for seed formation is important factor determining the nanoparticle size and its size distribution. As the seeds are rapidly formed during short period, size of nanoparticle becomes small and size distribution becomes narrow. Because the radical species is more reactive than aldehydes for the reduction process, seeds are formed in new glycerol rapidly more than in old glycerol. Rapid seed formation in new glycerol could lead to the formation of small nanoparticles and narrow size distribution.
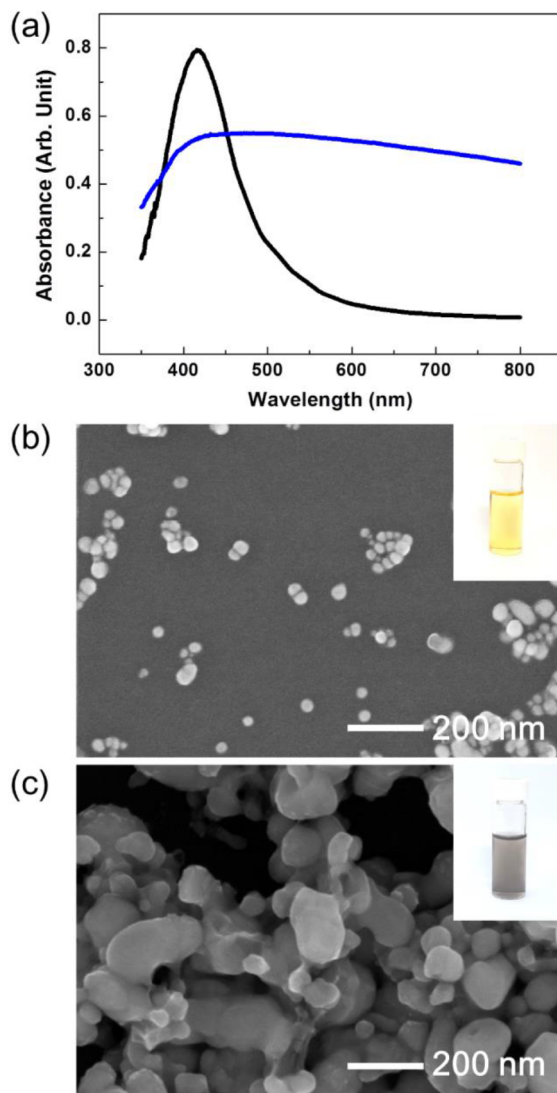
Figure 7: Silver nanoparticles with homogeneous size distribution are synthesized by radicals as represented by black line in (a) and electron micrograph, (b). On the other hand, when the silver nanoparticles are formed by aldehyde, their size distribution is wide as shown in blue line in (a) and electron micrograph, (c).

4.   Conclusion

In this paper, we report unprecedented synthesis of silver nanoparticles in glycerol in which no extra energy and chemical additives are needed, and all chemical reaction is performed at room temperature in neutral pH condition. Many research papers have reported the synthesis of silver nanoparticles in glycerol, but they are mostly prepared under extreme condition, e.g., high temperature, ultraviolet light, or alkaline pH condition. Because this is the first example demonstrating the synthesis of silver nanoparticles in glycerol under normal condition, the synthetic mechanism should be different with those generally accepted. Moreover, it is found that silver ions are reduced by two different chemical species in glycerol as a result of mechanistic study. One species is glyceraldehydes converted from glycerol by dissolving oxygens, and the other one is free radicals generated from glycerol mainly by ambient thermal energy. The concentration of free radicals is dependent on the amount of aldehydes, because aldehydes could play the role as scavengers of free radicals. The interesting thing is that the nanoparticle's size and its distribution are dependent on the reducing chemical species. When silver ions are reduced mainly by aldehydes, large nanoparticles are formed and their size distribution is wide, however, when reduced by free radicals, small nanoparticles with narrow size distribution are obtained. According to our experiment result, small silver nanoparticles with narrow size distribution can be synthesized in glycerol, but the glycerol should not contain aldehydes (e.g., glyceraldehydes). If we can effectively remove aldehydes from the glycerol that have been exposed to air for a long time, it is expected that small nanoparticles with narrow size distribution should be prepared even in old glycerol produced long ago.

III. In Situ Syntheses of Silver Nanoparticles Inside Silver Citrate Nanorods via Catalytic Nanoconfinement Effect

1. Introduction

It has been known for a long time that silver ions (salts) have antimicrobial properties, and silver nitrate and its aqueous solutions have been used for wound and ulcer treatments since the 17th century[35] . Conversely, the antimicrobial properties of silver nanoparticles have only begun to be reported relatively recently with the development of techniques for nanomaterial syntheses[36], [37] . There has been general agreement on the bactericidal activity of silver ions/salts; however, there is still debate as to which chemical species (silver ions released from the silver nanoparticles or the silver nanoparticles themselves) exhibit these bactericidal properties[38], [39] . Several studies have shown that silver ions released from silver nanoparticles are the main contributors of the antimicrobial properties[40]–[44] ; however, other papers have reported that the toxicity of silver nanoparticles is not entirely due to released silver ions[36], [45], [46] . The enhanced antimicrobial activity of silver nanoparticles is most likely due to reactive oxygen species generated from the surface of the nanoparticles [47] or direct interactions of the particles with the cell membranes of microbes[48], [49] . Although the underlying antimicrobial mechanism is not yet clear, many consumer products related to silver nanoparticles are commercially available [50]. Silver nanoparticles have several advantages over silver ions/salts, despite released silver ions being the main agents of their bactericidal properties. The surfaces of silver nanoparticles act as reservoirs for the release of silver ions at

29

a limited rate; therefore, silver ions can be provided at a desirable rate without instant overdose. Additionally, since silver ions can be adsorbed onto and released from the surfaces of nanoparticles, silver nanoparticles can serve as a vehicle for effective delivery of silver ions to the vicinity of microbes[36], [42] . Thus, silver ions can be easily approach to target microbes without interference from native ions (Cl^- or S^{2-}) in the body[51] and can be effectively released by local acidic pH in the proximity of the cell membranes of microbes, resulting in enhanced antimicrobial activities[52] . Despite these benefits, it is problematic to apply these particles directly to wound sites, because direct contact of silver nanoparticles with mammalian cells can lead to their destruction via cellular uptake or cell membrane damage[52], [53] . One of the proposed methods for avoiding this problem is to embed the nanoparticles in matrices such as hydrogels, polymers, or composites. Embedding makes nanoparticles resistant to oxidation and bacterial colonization and prevents them from being released and infiltrating the fluids or tissues of the body[54]–[60] . To date, numerous methods for fabricating silver nanoparticle-embedded antimicrobial materials have been introduced. These methods can be categorized into three groups: 1) adsorption of pre-synthesized silver nanoparticles in a matrix, 2) reduction of silver ions pre-adsorbed in a matrix by external reducing agents, and 3) pre-introduction of a reducing group into a matrix followed by adsorption and reduction of silver ions. In the first method, silver nanoparticles are pre-prepared, and subsequently adsorbed in a matrix (chitosan film or modified glass surface)[54], [55] . This method has limited applications for three-dimensional matrices due to silver nanoparticles being relatively large and unable to effectively infiltrate these matrices [61]. In the second method, silver ions are first adsorbed in a matrix that contains chemically active groups that are able to bind silver ions, subsequently

silver ions are reduced inside the matrix by addition of reducing agents [56], [58]. Since the silver ions are small enough to infiltrate the matrix, they are able to be uniformly adsorbed and result in silver nanoparticles being well dispersed inside the matrix. However, in this method, reducing agents must be added to the matrix to reduce the silver ions. In the third method, functional groups that are able to reduce silver ions are first introduced in the matrix, then the matrix is allowed to adsorb silver ions[59], [60] . The silver ions are reduced to silver nanoparticles inside the matrix without addition of reducing agents. In this method, although addition of reducing agents is unnecessary, an additional step of pre-functionalization of the matrix is required. In this study, we demonstrate two processes in which silver nanoparticles are formed inside silver citrate nanorods resulting in embedded silver nanoparticles. In the first process, silver nanoparticles are prepared inside silver citrate nanorods at much lower temperatures than those at which they are typically prepared. Generally, silver nanoparticles are produced in a bulk solution containing silver and citrate ions near the boiling temperature of water ($100°C$) due to their high activation energy. However, when silver and citrate ions are confined in a small space, such as the silver citrate nanorods used in this study, nanoparticles can be produced at much lower temperatures (as low as $25°C$). The second process demonstrates in situ generation of silver nanoparticles inside silver citrate nanorods via electron beam irradiation. Observations of silver citrate nanorods using transmission electron microscopy showed that silver nanoparticles can be formed inside silver citrate nanorods using only two minutes of electron beam irradiation. The fundamental principles of the proposed efficient syntheses are also discussed in terms of the catalytic effect of reactants confined in nanospaces[62], [63]

31

2.   Experimental

2. 1.   In Situ Syntheses of Silver Nanoparticles Inside Silver Citrate Nanorods

Silver nanoparticles were generated in situ inside of silver citrate nanorods pre-prepared using a previously published procedure . In general, the nanorods were prepared using two solutions [silver nitrate (0.2 M, aq) and trisodium citrate dihydrate (0.2 M, aq)] composed of deionized water (18.2 MΩ·cm) and silver nitrate (AgNO3; 99.0%; Sigma-Aldrich, Seoul, Republic of Korea) or trisodium citrate dihydrate (TSC, C6H5Na3O72H2O; 99.0%; OCI, Ltd., Seoul, Republic of Korea). Upon mixing, the two initially transparent solutions turned into a white opaque mixture; indicating the formation of silver citrate compounds. After mixing, the solutions were further mixed at 340 rpm for 30 min at ambient temperature (25 °C). The mixture remained opaquely white; however, the morphology of the silver citrate compounds changed from irregular-shaped micron-sized particles to nanorods 1.3 m in length and 130 nm in diameter. The dimensions of the nanorods were variable based on stirring rate and time over a wide range. When the pre-synthesized silver citrate nanorods were heated over the range of room temperature (25°C) to 92C, the color of the solution containing the nanorods changed from opaque white to brown; indicating the formation of silver nanoparticles. Synthesis of silver nanoparticles was restricted to the interior of the silver citrate nanorod matrix, while the exterior remained as nanorods. Although temperature did not affect the formation of the nanoparticles, it did affect the rate of formation. For example, silver nanoparticles could be formed inside silver citrate nanorods over several hours at 60°C, but took several days at room temperature (25°C). Silver nanoparticles were also synthesized in situ

32

inside silver citrate nanorods via electron beam irradiation in a transmission electron microscope chamber. In this method, white opaque solutions containing silver citrate nanorods were loaded onto gold grids, which are more chemically stable than copper. When an electron beam, accelerated at 200 kV at a density of 5 mA/cm2, using transmission electron microscopy (TEM, JEM-ARM200 with Cold FEG; JEOL, Ltd., Tokyo, Japan) was irradiated onto the silver citrate nanorods over several minutes (3 min), silver nanoparticles were formed exclusively inside the silver citrate nanorods, as observed in bright field images.

2. 2. Characterization of the In Situ Synthesized Silver Nanoparticles Inside Silver Citrate Nanorods

The outer morphology of the silver citrate nanorods prepared with and without heating was investigated using scanning electron microscopy (SEM; S-4800; Hitachi, Tokyo, Japan). A drop of each solution was loaded onto a clean Si wafer, then dried and washed with deionized water to remove organic residues. For improved observation, platinum was coated onto the samples via a plasma sputter coater (E-1030; Hitachi, Tokyo, Japan). The inner structures of the samples were observed using TEM (JEM-F200; JEOL, Ltd., Tokyo, Japan) at an acceleration voltage of 200 kV on a gold grid. Oxygen plasma (CUTE; Femto Science, Inc., Hwaseong-si, Republic of Korea) or furnace (Muffle Furnace 62700; Barnstead International, Inc., Iowa, USA) treatment was used to remove the organic portions of the samples. Oxygen plasma treatment was performed at full power (100 W) for several minutes with samples loaded onto glass slides. Thermal treatment was performed at 150 or 300 C for 15 or 30 min, respectively. Before and after thermal treatment, the sample compositions were analyzed for remaining residues using

an electron dispersive spectrometer (EDS) coupled to the SEM. The number of silver nanoparticles formed inside the silver citrate nanorods was monitored using an UV-Vis spectrophotometer (Optizen 3220UV; MECASYS, Co., Ltd., Daejeon, Republic of Korea) of fixed path length (1 cm) with disposable cuvettes. The white and brown colloidal solutions were so concentrated that they were not transparent enough for measurement. Therefore, dilutions were made to the point where scattering minimally affected the spectra while absorbance remained high. The absorbance at each reaction time was obtained via surface plasmon resonance, and the area below each maximum peak absorbance was integrated. The chemical identity of the organic matrix was investigated using a Fourier-transform infrared (FTIR) spectrometer (NICOLET 6700; Thermo Fisher Scientific, Seoul, Republic of Korea) in transmission mode with KBr. The ratio of KBr to sample was 100:1 w/w, and the number of scans was 200 for an increased signal to noise ratio.

3.   Results and Discussion

In our previous paper[64] , we reported that silver citrate nanorods can be easily synthesized by mechanical stirring. Specifically, when two aqueous solutions [Figure 1(a) and (b)] are mixed under mechanical stirring at 340 rpm at room temperature (25°C), a white colloidal solution is immediately formed, as shown in Figure 1(c). The morphology of the colloid particles contained in the white solution has been verified as nanorods [Figure 1(d)], and their chemical composition revealed as silver citrate . When the white colloidal solution is heated at 60 °C for several hours, its color drastically changes to brown, as shown in Figure 1(e). This color change can also occur at room temperature (25°C), but

takes several days to turn brown. The change in color of the solution from white to brown means that various shapes of silver nanoparticles (typically spherical or rod shaped) are synthesized and contained in the solution. This color change is rather surprising because silver nanoparticles usually cannot be made at such low temperatures (25–60°C) using citrate ions. Synthesis of silver nanoparticles using citrate ions is a well-established, traditional method; however, the reaction is most often performed near the boiling temperature of water (100°C)[65], [66]. Another interesting observation is that there is no major difference between the morphology of the brown and white colloid particles. As shown in Figure 1(f), the colloid particles in the brown solution have the same morphology as the nanorods in the white solution, despite having completely different colors.

To explore the source of the brown coloration, the brown colloidal solution was filtered using a 2-μm pore-diameter filter paper (Supporting Figure 1). The color of the filtrate was transparent, and no characteristic peak representing silver nanoparticles was observed in the spectral range of 400500 nm [Supporting Figure 1(e)]. The color of the residue [Supporting Figure 1(b)] was brown; the same color as the original solution [Supporting Figure 1(a)]. The morphology of the residue [Supporting Figure 1(d)] was nanorods, the same as that shown in Figure 1(f), and no spherical-shaped particles were observed. This result indicates that the nanorods shown in Figures 1(f) and 2(d) could be either silver nanorods or various shaped silver nanoparticles embedded inside the nanorods.

The residue was further investigated using TEM, yielding structural differences between the white [Figure 1(d)] and brown [Figure 1(f)] nanorods. Although both nanorods showed similar morphologies when viewed under SEM, their inner structures observed under TEM were completely different, as represented in figure 9(a) and (b). In comparison to figure 9(a), showing the TEM image of the
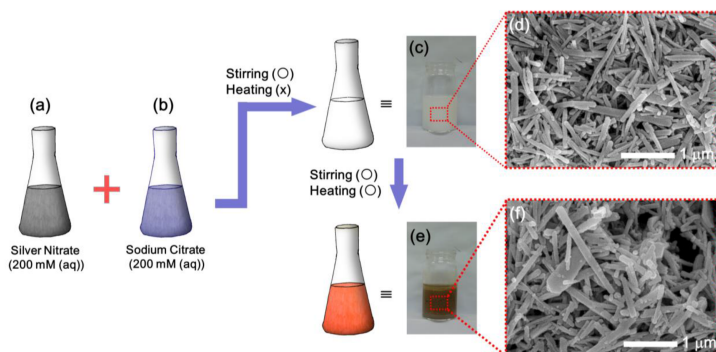
Figure 8: Silver citrate nanorods prepared by mixing (a) silver nitrate solution (200 mM, aq) with (b) sodium citrate solution (200 mM, aq) via mechanical stirring at 340 rpm at room temperature (25°C). (c) Color of the colloidal solution is white and (d) morphology of the silver citrate is nanorods. (e) When the white colloidal solution is heated, its color changes to brown, (f) but the morphology of the colloids remains unchanged. (○) with and (x) without treatment.

white nanorods, the brown nanorods contained many nanoparticles [figure 9(b)]. This difference is more clearly distinguished in the highlighted images (insets with white dotted lines). Nanoparticles are not observed in the inset of figure 9(a), but many nanoparticles of 10 nm in diameter are clearly seen in the inset of figure 9(b).

We hypothesized that these nanoparticles were the source of the brown coloration of the nanorods, which were expected to be silver. To clarify this, high-resolution TEM images and selective area electron diffraction patterns were obtained and analyzed as shown in figure 9(c) and (d) and the inset of (c).

36
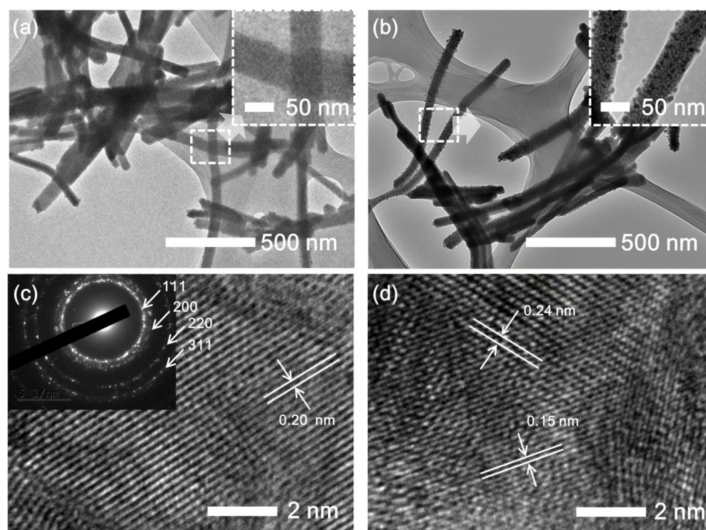
Figure 9: Transmission electron microscopy (TEM) images of the inner structures of the nanorods present in (a) white and (b) brown colloidal solutions. The areas highlighted with white dashed lines in each image are magnified in the insets to clarify the differences between the nanorods. (c and d) High-resolution TEM images of the lattice spacing and [inset of (c)] ring pattern of the nanoparticles formed inside the silver citrate nanorods in (b), which are representative of silver nanoparticles.

The distance between each ring pattern and the center correspond well with the reciprocal inter-atomic spacing of each lattice plane of silver [figure 9(c), inset], and the 0.20 nm measurement corresponds to the inter-atomic spacing of the 200 plane of silver. Further inter-atomic spacing measurements, 0.24 and 0.15 nm, corresponding to 111 and 220 of silver, respectively, were also observed in a different facet [figure 9(d)]. The composition of the brown nanorods was

37

also identified using energy dispersive spectroscopy (figure 10). As predicted from figure 9, traditional silver peaks appeared at 2.64, 3.00, and 3.16 keV in the energy dispersive spectrum (figure 10). In addition to silver peaks, a number of smaller peaks were observed between 0.40 and 2.00 keV. For clearer observation of these smaller peaks, the spectral region between 0.40 and 2.00 keV was magnified (highlighted with a red dotted box), as shown in the inset of figure 10. Carbon and oxygen peaks, shown at 0.26 and 0.52 keV, respectively, are presumably elements composing the nanorod matrix. The copper signals, appearing at 0.92, 8.04, and 8.92 keV, are from the copper grid used for the TEM measurements. The two peaks at 1.24 and 1.42 keV were assigned as escape peaks, which are traditional artifacts in EDS, because these peaks are red-shifted from the silver peaks (3.00 and 3.16 keV) by exactly the difference of Si K-shell X-ray energy (1.74 keV). The broad, small peak near 1.74 keV is another artifact known as the Si internal fluorescence peak, originating from the dead layer of the Si detector . A small peak corresponding to Na Kα is also shown at 1.04 keV, which indicates that a small amount of silver ions in the brown nanorods were replaced with sodium ions originating from the trisodium citrate dihydrate.

Based on these experimental results, we tentatively concluded that the brown nanorods consisted of an organic matrix composed of carbon and oxygen with embedded silver nanoparticles. To confirm this, we treated the brown nanorods to three different processes. First, the nanorods were treated with oxygen plasma; a conventional technique used to remove organic impurities or contaminants from the surfaces of substrates. If the matrix was composed of organic substances, these would be easily removed through oxidation via oxygen plasma treatment. We expected that the organic matrix would be removed from the brown nanorods by oxygen plasma; however, metal nanoparticles still remained. After plasma
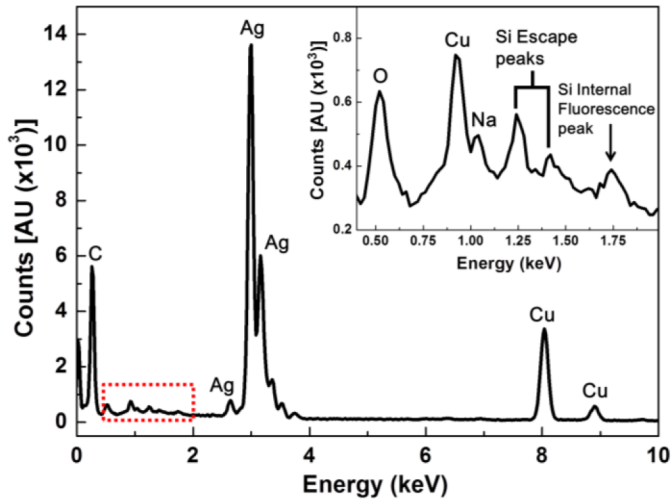
Figure 10: Energy dispersive spectrum of figure 9(b) representing that the formed nanoparticles inside the silver citrate nanorods are silver nanoparticles. The small peaks between 0.4 and 2.0 keV are assigned in the inset.

treatment for 1 min [figure 11(a)], it was observed that the matrix of the brown nanorods was removed, but the nanoparticles still remained and arranged as nanorods. Despite the plasma treatment being prolonged to 3 and 5 min, the nanoparticles, aligned as nanorods, were not removed [figure 11(b) and (c), respectively]. The same phenomenon was also observed with heat treatment; another method for effectively removing organic substances [figure 11(d) and (e)]. When brown nanorods were treated in a furnace at 150°C for 15 min,

only the matrix of the brown nanorods was removed, leaving the nanoparticles arranged as nanorods [figure 11(d)]. When the brown nanorods were treated in the same furnace at a higher temperature (300°C) for a longer period (30 min), the nanoparticles remained [figure 11(e)] like those in the oxygen plasma treatment. The composition of the remaining material after heat treatment was analyzed by EDS, and was revealed to be silver as expected.

Since the chemical composition of the white nanorods is silver citrate and citrate ions are capable of reducing metal ions, the silver ions should be reduced by the citrate ions to form nanoparticles inside the nanorods. According to several reports[65], [67], [68] , after citrate ions reduce metal ions they are transformed into acetone-1,3-dicarboxylates as shown in Eq. (1):
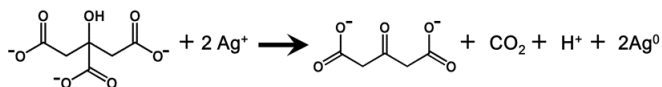
Before and after the reaction, the alcohol group disappears and a ketone group is formed. Because both vibrational modes (C-O of 3rd alcohols and C=O of ketones) are IR active, we expected that the structural change in the citrate ions would be detectable in IR spectra. IR spectra of both samples (white and

40
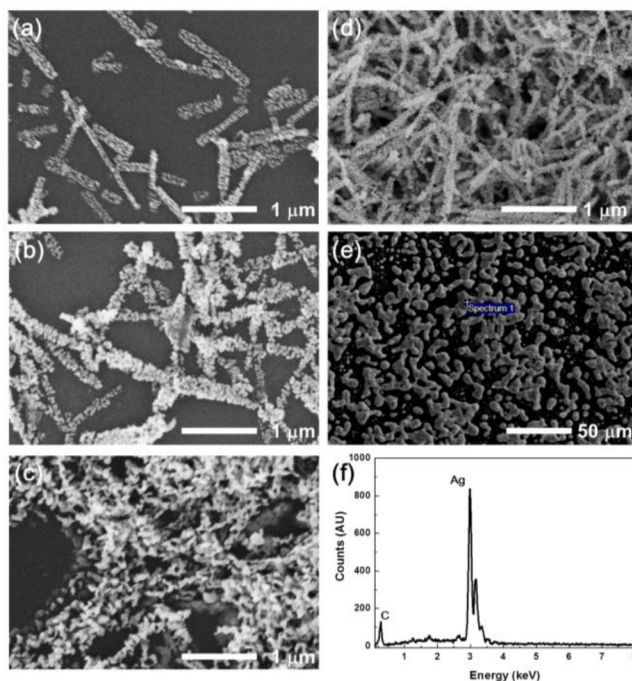
Figure 11: Time-dependent scanning electron microscopy images of the nanorods contained in the brown colloidal solution after oxygen plasma treatment for (a) 1, (b) 3, and (c) 5 min; and heat treatment in a furnace at (d) 150°C for 15 min and (e) 300°C for 30 min. (f) Energy dispersive spectrum measured at the point designated as "Spectrum 1" in (e), representing that the residues after heat treatment are silver.

brown nanorods) were obtained and compared. In figure 12, the red and black lines are spectra of white (before reaction) and brown (after reaction) nanorods,

41
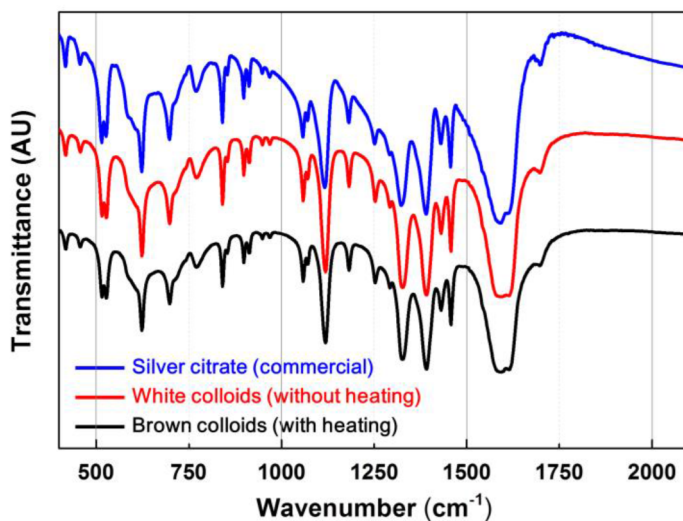
Figure 12: Fourier-transform infrared spectra of the nanorods contained in the white (red) and brown (black) colloidal solutions. These spectra have identical profiles to that of commercially purchased silver citrate (blue).

respectively.

According to Eq. (1), ketones are only formed after the reaction, so the peak at 1715 cm^{-1}, corresponding to the carbonyl stretching mode of a ketone, should only be present for the brown nanorods (figure 12, black line); however, only a small peak around 1700 cm^{-1}, rather than 1715 cm^{-1}, was observed.

42

In addition, the peak at 1700 cm^{-1} not only appeared in the spectrum of the brown nanorods but also in that of the white nanorods. This peak is most likely representative of the carbonyl stretching mode of a carboxylic acid, which typically appears around 1710 cm^{-1}. Some of the carboxylates in the citrate ions and acetone-1,3-dicarboxylates may be in the form of carboxylic acids. The carbonyl stretching mode of ketones overlaps that of carboxylic acids, and therefore may not appear in the results. Meanwhile, the C-O stretching mode (1120 cm^{-1}) corresponding to 3rd alcohols was only expected to be present in the spectrum of the white nanorods (red line) and disappear in that of the brown nanorods (black line) because the alcohol group is removed after the reaction. Contrary to our expectation, both spectra contained representative C O stretching modes at 1120 cm^{-1}. Also notable was not only that the spectra of the white and brown nanorods were nearly identical, but that they closely resembled that of commercially purchased silver citrate (figure 12, blue line). Although these results are not yet clearly explained, they may be due to a high concentration of citrate ions that were not converted to ketones during the reduction of the silver ions. Based on these experimental results, we think that the brown nanorod matrix consists of a large concentration of citrate ions and small concentration of acetone-1,3-dicarboxylate ions, even after the reduction of the silver ions. As depicted in Scheme 1, the main composition of the white nanorods is silver citrate, in which some of the carboxylates are in the form of carboxylic acids. After the reaction, some of the citrate ions are converted into acetone-1,3-dicarboxylates and the silver ions are reduced, resulting in the formation of silver nanoparticles inside the brown nanorods; however, a large concentration of citrate ions still remain inside the brown nanorods. As mentioned, the reduction of silver ions and formation of silver nanoparticles occur exclusively inside the

nanorod matrix at low temperatures. This phenomenon can be explained by the catalytic effect in small spaces. Because citrate and silver ions are confined in small spaces, such as those of the nanorod matrix, their reduction and oxidation can be accelerated (catalytic nanoconfinement effect).
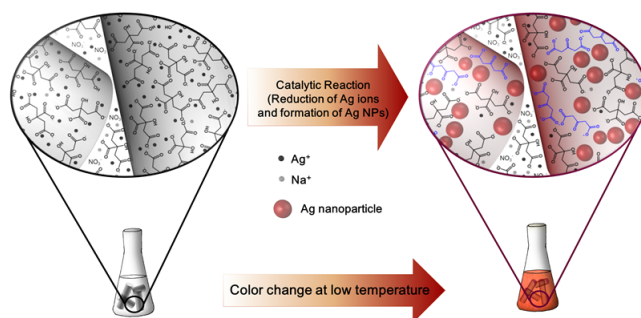
Scheme 3. Silver nanoparticles (NPs) exclusively formed inside the silver citrate nanorods at low temperatures due to the catalytic nanoconfinement effect

Since the absorbance near the surface plasmon resonance energy of silver nanoparticles is proportional to the number of nanoparticles produced, the activation energy lowered by catalytic nanoconfinement effect can be estimated using time-dependent absorption spectra taken at different temperatures. As the reaction progressed at different temperatures (64, 70, 80, and 92°C), the coloration change of the nanorods from white to brown was monitored using UV-Vis absorption spectroscopy (Supporting figure 9). In general, the rates of most of the chemical reactions accelerated at higher temperatures, because the number of reactants possessing energy beyond activation energy increased as thermal energy was applied. As expected, the time required for the white nanorods to turn brown decreased as reaction temperature increased.
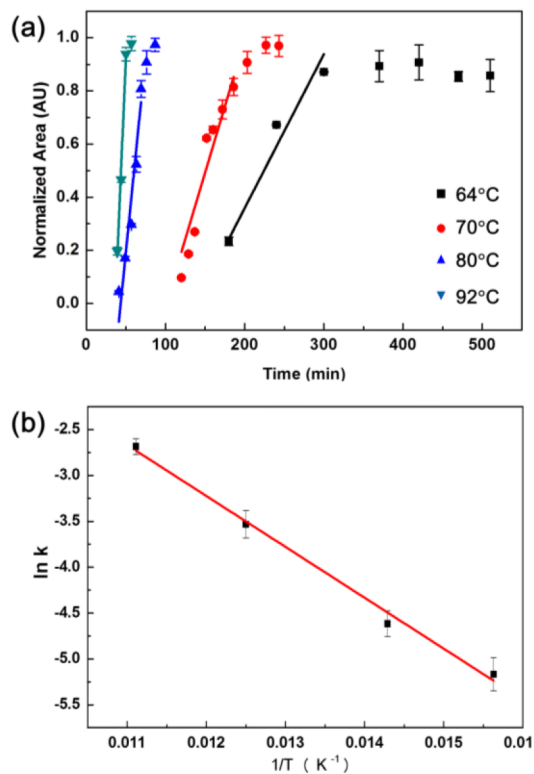
Figure 13: (a) Kinetic measurements of the color change of the nanorods at 64 (black square), 70 (red circle), 80 (blue triangle), and 92°C (green inverted triangle). (b) Arrhenius plot of the kinetic data in (a).

Specifically, the coloration of the white colloidal solution did not fully change to brown at 64°C, until the reaction reached 300 min, represented by black squares in figure 13(a). This reaction period was shortened by 100 min, from 300 to 200 min, when the temperature was increased from 64 to 70°C. The higher the reaction temperature, the shorter the reaction period. The reaction rate

at each temperature was obtained from the slopes of the curves in figure 13(a), yielding values of 0.006 ± 0.001, 0.010 ± 0.001, 0.030 ± 0.004, and 0.068 ± 0.006 min$_{-}1$ for 64, 70, 80, and 92°C, respectively. Assuming an Arrhenius-type reaction rate, the activation energy was estimated from the slope of the graph [figure 13(b)] in which the natural logarithm of each rate constant was plotted as a function of inverse temperature. Since the reduction of silver ions by citrate ions typically occurs at high temperatures, such as those near the boiling temperature of water, the activation energy of the reaction is high (several hundred kJ/mol) [68]. However, in this experiment, the obtained activation energy was 4.61 ± 0.26 kJ/mol. This lowered activation energy is thought to be the result of the small space confinement of silver and citrate ions leading to facilitated electron transfer (reduction and oxidation) and agglomeration of silver atoms (nucleation and growth of silver nanoparticles).

Silver nanoparticles were also synthesized in situ by electron beam irradiation. During our investigation of the white nanorods using an electron beam in a TEM chamber, we observed that silver nanoparticles were formed inside the nanorod matrix. When the white nanorods were exposed to an electron beam for only 1 min, nanoparticles were not generated [figure 14(a) and (b)]. However, when electron beam irradiation was prolonged to 3 min, nanoparticles began to be generated inside the nanorod matrix, as shown in figure 14(c). Once the nanoparticles were formed after 3 min of irradiation, further irradiation did not generate further formation of particles [figure 14(d)]. This process can be clearly observed in the magnified images, highlighted with black squares, in figure 14. Through close observation of figure 14(a-1) and (b-1), it can be seen that the uniform contrast inside the nanorod begins to change to non-uniform contrast within 1 min of irradiation. When the electron beam is irradiated for 3 min,

nanoparticles are rapidly generated inside the nanorod matrix [figure 14(c-1)]. Once a mass of nanoparticles is formed inside the matrix, further nanoparticle generation is impeded [figure 14(d-1)].
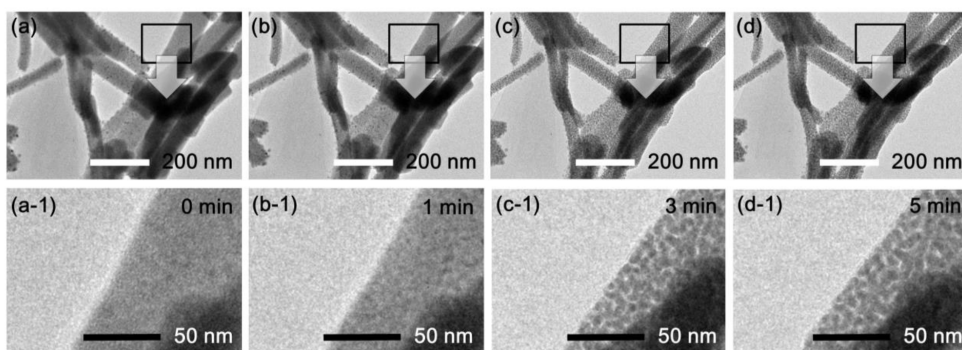
Figure 14: Time-dependent transmission electron microscopy (TEM) images taken at (a) 0, (b) 1, (c) 3, and (d) 5 min after electron beam irradiation in a transmission electron microscope chamber. Silver nanoparticles are rapidly formed inside the silver citrate nanorods after 3 min of electron beam irradiation.

Electron beam-induced syntheses of metal nanoparticles have already been reported by several research groups , and which can be divided into two categories. In one category, metal precursors (ions) solubilized in bulk aqueous solutions were reduced by reactive chemical species (hydrogen or hydroxide radicals) generated by relatively strong electron beams in electron

beam accelerators [69], [70]. In the other category, metal nanoparticles were synthesized in limited small spaces such as zeolites, metal-organic frameworks, or polymers via relatively weak electron beams using electron microscopy [71], [72]. In the latter studies, because metal precursors were confined to small spaces, they can be easily reduced, and the reduced metal atoms can be easily aggregated (catalytic nanoconfinement effect). Therefore, syntheses of metal nanoparticles within limited spaces was performed in a transmission electron microscope chamber with a few hundred keV, which is smaller than the electron energy of an electron beam accelerator (a few tens of MeV) by a factor of 10-100. Although further experiments are required to elucidate our facile, in situ synthesis of silver nanoparticles inside a silver citrate matrix by relatively low energy electron beam, this phenomenon is most likely related to the catalytic nanoconfinement effect on the silver citrate nanorods.

4.   Conclusions

Silver nanoparticles remain useful materials in the field of antimicrobial agents despite controversy over the origin of their intrinsic antimicrobial properties. Silver nanoparticles can not only be used as antimicrobial agents, but can also serve as materials for enhancing the activities of other antimicrobial agents. They have the capabilities of serving as reservoirs for continuous release of silver ions and for use as a vehicle for delivery of antimicrobial agents. The prerequisites for silver nanoparticles in such applications include their restricted dispersal and release in regions they are applied and chemical stability of their surfaces. The best way to ensure these characteristics is to embed silver nanoparticles in a matrix. In this study, we demonstrated that silver nanoparticles can be facilely and

in situ synthesized inside silver citrate nanorods, which have been shown to serve as antimicrobial agents in our previous paper. Silver nanoparticles were formed inside the silver citrate nanorods at low temperatures (as low as 25°C), compared to the high temperatures typically used in bulk solutions, and by electron beam irradiation using a low dose rate. These results are explained by the enhanced redox reaction and growth rates of metal ions and atoms, respectively, as a result of the catalytic nanoconfinement effect. It is expected that the silver nanoparticle-embedded silver citrate nanorods prepared in this study will show enhanced antimicrobial properties in terms of long-lasting and/or sustained-release agents.

REFERENCES

[1] C. J. R. C. J. A. J. Quispe C. A. G.; Coronado, "Glycerol: production, consumption, prices, characterization and new trends in combustion," *Sust. Energ. Rev*, vol. 27, pp. 475–493. 2013.

[2] J. H. A. S. R. K. M. T. P. B. B. M. A. S. Monisha, "Biodiesel: a review.," *Int. J. Eng. Re*, vol. 6, pp. 902–912. 2013.

[3] R. K. H. R. M. P. C. D. Pagliaro M.; Ciriminna, "From glycerol to value-added products.," *Angew. Chem. Int. Ed*, vol. 46, pp. 4434–4440. 2014.

[4] C. D. R. M. Ciriminna R.; Pina, "Pagliaro M. Understanding the glycerol market.," *Eur. J. Lipid Sci. Technol.*, vol. 116, pp. 1432–1439. 2014.

[5] A. S. A. B. A. Bagnato G.; Iulianelli, "Glycerol production and transformation: a critical review with particular emphasis on glycerol reforming reaction for producing hydrogen in conventional and membrane.," *reactors. Membranes*, 2017,7,17.

[6] A. E. Vaidya P. D.; Rodrigues, "Glycerol reforming for hydrogen production: a review.," *Chem. Eng. Technol.*, vol. 32, pp. 1463–1469. 2009.

[7] C. S. Y. Wolfson A.; Dlugy, "Glycerol as a green solvent for high product yields and selectivities.," *Environ. Chem. Lett.*, vol. 5, pp. 67–71. 2007.

[8] S. J. Clark J. H.; Tavener, "Alternative solvents: shades of green.," *Org. Process Res. Dev.*, vol. 11, pp. 149–155. 2007.

[9] V. Díaz-Álvarez A. E.; Cadierno, "Glycerol: a promising green solvent and reducing agent for metal-catalyzed transfer hydrogenation reactions and nanoparticles formation.," *Appl. Sci.*, vol. 3, pp. 55–69. 2013.

[10] F. Gu Y.; Jérôme, "" *Green Chem*, vol. 12, pp. 1127–1138. 2010.

[11] B. P. Sinha A.; Sharma, "Preparation of copper powder by glycerol process.," *Mater. Res. Bull.*, vol. 37, pp. 407–416. 2002.

[12] ——, "Preparation of silver powder through glycerol process.," *Bull. Mater. Sci.*, vol. 28, pp. 213–217. 2005.

[13] K. H. C.-S. Ullah M. H.; Il, "Preparation and optical properties of colloidal silver nanoparticles at a high Ag+ concentration.," *Mater. Lett.*, vol. 60, pp. 1496–1501. 2006.

[14] K. Grace A. N.; Pandian, "One pot synthesis of polymer protected gold nanoparticles and nanoprisms in glycerol.," *Colloids Surf. A Physicochem. Eng. Asp.*, vol. 290, pp. 138–142. 2006.

[15] ——, "One pot synthesis of polymer protected Pt, Pd, Ag and Ru nanoparticles and nanoprisms under reflux and microwave mode of heating in glycerola comparative study.," *Mater. Chem. Phys.*, vol. 104, pp. 191–198. 2007.

[16] K. Nisaratanaporn E; Wongsuwan, "Preparation of ultrafine silver powder using glycerol as reducing agent.," *J. Met. Mater. Min.*, vol. 18, pp. 1–5. 2008.

[17] B. J. K.-M. F. E. V. X. Y. Skrabalak S. E.; Wiley, "On the polyol synthesis of silver nanostructures: glycoaldehyde as a reducing agent ," *Nano Lett.*, vol. 8, pp. 2077–2081. 2008.

[18] C.-Y. Chou K.-S.; Ren, "Synthesis of nanosized silver particles by chemical reduction method.," *Mater. Chem.*, vol. 64, pp. 241–246. 2000.

[19] J. P. B. B. Fievet F.; Lagier, "Homogeneous and heterogeneous nucleations in the polyol process for the preparation of micron and submicron size metal particles.," *Solid State Ion.*, vol. 32/33, pp. 198–205. 1989.

[20] G. S. Y.-L. Z. H. D. E. P. Benet W. E.; Lewis, "The mechanism of the reaction of the Tollens reagent.," *J. Chem. Res.*, vol. 135, pp. 675–677. 2011.

[21] S. M. T. Sarkar A.; Kapoor, "Synthesis and characterization of silver nanoparticles in viscous solvents and its transfer into non-polar solvents.," *Res. Chem. Intermed.*, vol. 36, pp. 411–421. 2010.

[22] S. N. E. Preuksarattanawut T.; Asavavisithchai, "Fabrication of silver hollow microspheres by sodium hydroxide in glycerol solution.," *Mater. Chem. Phys.*, vol. 130, pp. 481–486. 2011.

[23] T. K. S. Nalawade P.; Mukherjee, "Green synthesis of gold nanoparticles using glycerol as a reducing agent.," *Adv. Nanoparticle.*, vol. 2, pp. 78–86. 2013.

[24] G. O. M. O.-C. K. O. Genç R.; Clergeaud, "Green synthesis of gold nanoparticles using glycerol-incorporated nanosized liposomes.," *Langmuir*, vol. 27, pp. 10 894–10900. 2011.

[25] A. C. G. J. F. T.-F. G. Gasparotto L. H. S.; Garcia, "Electrocatalytic performance of environmentally friendly synthesized gold nanoparticles towards the borohydride electro-oxidation reaction.," *J. Power Sources*, vol. 218, pp. 73–78. 2012.

[26] L. H. S. G. J. F. T.-F. G. Garcia A. C.; Gasparotto, "Straightforward synthesis of carbon-supported Ag nanoparticles and their application for the oxygen reduction reaction.," *Electrocatal.*, vol. 3, pp. 147–152. 2012.

[27] W.-S. A. K. H. K. D. S. L. H.-S. L. Y.-W. Kim M.; Son, "Hydrothermal synthesis of metal nanoparticles using glycerol as a reducing agent.," *J. Supercrit. Fluid.*, vol. 90, pp. 53–59. 2014.

[28] A. C. F. E. B. P. C. O. V. L. T.-F.-G. G. L. H. S. Gomes J. F.; Garcia, "New insights into the formation mechanism of Ag, Au and AgAu nanoparticles in aqueous alkaline media: alkoxides from alcohols, aldehydes and ketones as universal reducing agents.," *Phys. Chem. Chem. Phys.*, vol. 17, pp. 21 683–21693. 2015.

[29] G. H. B. Huang Z. Y.; Mills, "Spontaneous formation of silver particles in basic 2-propanol.," *J. Phys. Chem.*, vol. 97, pp. 11 542–11550. 1993.

[30] S.-P. L. J. K. Jo J.; Cho, "Template synthesis of hollow silver hexapods using hexapod-shaped silver oxide mesoparticles.," *J. Colloid. Interface Sci.*, vol. 448, pp. 208–214. 2015.

[31] B. C. Smith, "Alcohols-the rest of the story.," *Spectroscopy*, vol. 32, pp. 19–23. 2017.

[32] S. I. A. A. Yaylayan V. A.; Harty-Majors, "Investigation of DL-glyceraldehyde-dihydroxyacetone interconversion by FTIR spectroscopy.," *Carbohydr. Res.*, vol. 318, pp. 20–25. 1999.

[33] D. G Forney C. F.; Brandl, "Control of humidity in small controlled-environment chambers using glycerol-water solutions.," *Technol. Product Rep.*, vol. 2, pp. 52–54. 1992.

[34] C. J. Volk A.; Kähler, "Density model for aqueous glycerol solutions.," *Exp. Fluids*, vol. 59, p. 75. 2018.

[35] H. J. Klasen., "Historical review of the use of silver in the treatment of burns.," *I. Early uses, Burns* ., vol. 26, pp. 117–130. 2000.

[36] B. E. B. P. C. M. A. M. W. J. R.-J. L. E. S. B. L. Yin Y. Cheng, "More than the ions: The effects of silver nanoparticles on lolium multiflorum.," *Environmental Science Technology* ., vol. 43, pp. 7285–7290. 2009.

[37] L. A. P. Z. R. T. J. C. T. S. M. C. Aymonier U. Schlotterbeck, "Hybrids of silver nanoparticles with amphiphilic hyperbranched macromolecules exhibiting antimicrobial properties . , journal=Chemical Communications . , volume=24, pages=3018-3019., year=2002,"

[38] E. K. J. R. A. - 128) G. B.-P. A. Kedziora M. Speruda, "Similarities and differences between silver ions and silver in nanoforms as antibacterial agents.," *International Journal of Molecular Sciences* ., vol. 19, pp. 444–461. 2018.

[39] J. M. S. S. Pal Y. K. Tak, "Does the antibacterial activity of silver nanoparticles depend on the shape of the nanoparticle? a study of the gram-negative bacterium escherichia coli.," *Applied and Environmental Microbiology* ., vol. 73, pp. 1712–1720. 2018.

[40] R. H. H. J. Liu, "Ion release kinetics and particle persistence in aqueous nano-silver colloids.," *Environmental Science Technology* ., vol. 44, pp. 2169–2175. 2010.

[41] J. D. M. K. M. E. S. Kittler C. Greulich, "Toxicity of silver nanoparticles increases during storage because of slow dissolution under release of silver ions.," *Chemistry of Materials* ., vol. 22, pp. 4548–4554. 2010.

[42] H. L. P. V. L. C.-P. J. J. A. Z.-M. Xiu Q.-B. Zhang, "Negligible particle-specific antibacterial activity of silver nanoparticles.," *Nano Letters* ., vol. 12, pp. 4271–4257. 2012.

[43] C. S. L. R.-G. J. M. G.-C. M. V.-R. M. K. M. E. K. Loza J. Diendorf, "The dissolution and biological effects of silver nanoparticles in biological media.," *Journal of Materials Chemistry B* ., vol. 2, pp. 1634–1643. 2014.

[44] S. M. M.-M. A. J. L.-H. H.-K.-J. N. M. X. Yang A. P. Gondikas, "Mechanism of silver nanoparticle toxicity is dependent on dissolved silver and surface coating in caenorhabditis elegans .," *Environmental Science Technology* ., vol. 46, pp. 1119–1127. 2012.

[45] J. C. R.-J. R. L. J. Fabrega S. R. Fawcett, "Silver nanoparticle impact on bacterial growth: Effect of ph, concentration, and organic matter.," *Environmental Science Technology* ., vol. 43, pp. 7285–7290. 2009.

[46] B. W. F. M.-R. K. N. O.-L. S.-R. B. E. Navarro F. Piccapietra, "Toxicity of silver nanoparticles to chlamydomonas reinhardtii.," *Environmental Science Technology* ., vol. 42, pp. 8959–8964. 2008.

[47] H.-M. H.-P. C. R. H. Y. P. P. Fu Q. Xia, "Mechanisms of nanotoxicity: Generation of reactive oxygen species.," *Journal of Food and Drug Analysis* ., vol. 22, pp. 64–75. 2014.

[48] B. S.-S. I. Sondi, "Silver nanoparticles as antimicrobial agent: a case study on E. coli as a model for Gram-negative bacteria.," *Journal of Colloid and Interface Science* ., vol. 275, pp. 177–182. 2004.

[49] A. C.-K. H. J. B. K. J. T. R. M. J. Y. J. R. Morones J. L. Elechiguerra, "The bactericidal effect of silver nanoparticles.," *Nanotechnology* ., vol. 16, pp. 2346–2353. 2005.

[50] M. B. J. Pulit-Prociak, "Silver nanoparticles - a material of the future.," *Open Chemistry* ., vol. 14, pp. 76–91. 2016.

[51] C. J. M. T. D. W. S. Garg H. Rong, "Oxidative dissolution of silver nanoparticles by chlorine: Implications to silver nanoparticle fate and toxicity.," *Environmental Science Technology* ., vol. 50, pp. 3890–3896. 2016.

[52] S. V. S. Z. C. T. L. M. P. H. S. V. P. V. Asharani S. Sethu, "Investigations on the structural damage in human erythrocytes exposed to silver, gold, and platinum nanoparticles," *Advanced Functional Materials* ., vol. 20, pp. 1233–1242. 2010.

[53] C.-L. T. H.-J. Yen S.-H. Hsu, "Cytotoxicity and immunological response of gold and silver nanoparticles of different sizes," *Small* ., vol. 5, pp. 1533–1561. 2009.

[54] H. Y. G. S. Lu W. Gao, "Construction, application and biosafety of silver nanocrystalline chitosan wound dressing," *Burns* ., vol. 34, pp. 623–628. 2008.

[55] A. D.-G. D. L. M. D. C. L. C. M. V. A. P. P. P. L. V. A. Taglietti C. R. Arciola, "Antibiofilm activity of a monolayer of silver nanoparticles anchored to an amino-silanized glass surface," *Biomaterials* ., vol. 35, pp. 1779–1788. 2014.

[56] Y.-I. L. C. K. K. S. V. K. Rao P. R. Reddy, "Synthesis and characterization of chitosan-peg-ag nanocomposites for antimicrobial application," *Carbohydrate Polymers* ., vol. 87, pp. 920–925. 2012.

[57] C. L. S. H. H.-J. J. J. Song H. Kang, "Aqueous synthesis of silver nanoparticle embedded cationic polymer nanofibers and their antibacterial activity," *Applied Materials Interfaces* ., vol. 4, pp. 460–465. 2012.

[58] R. G. P. H.-M. G. López-Carballo L. Higueras, "Silver ions release from antibacterial chitosan films containing in situ generated silver nanoparticles .," *Journal of Agricultural and Food Chemistry* ., vol. 61, pp. 260–267. 2013.

[59] Z. W. Q. H. X. Huang X. Bao, "A novel silver-loaded chitosan composite sponge with sustained silver release as a long-lasting antimicrobial dressing.," *RSC Advances* ., vol. 7, pp. 34 655–34663. 2017.

[60] A. R. K. S.-M. S. R. G. T. Y. Y. J. S. N. P. M. D. W. C. H. P. C. S. K. A. GhavamiNejad A. R. Unnithan, "Mussel-inspired electrospun nanofibers functionalized with size-controlled silver nanoparticles for wound dressing application.," *Applied Materials Interfaces* ., vol. 7, pp. 12 176–12183. 2015.

[61] L. C. Y. L. B. X. R. B. W. W. L. J. Song P. Zhang, "Nano-silver in situ hybridized collagen scaffolds for regeneration on infected full-thickness burn skin," *Journal of Materials Chemistry B* ., vol. 3, pp. 4231–4241. 2015.

[62] D. S. S. V. R. J. R. B. S. M. A. G. S. Patra A. K. Pandey, "Redox decomposition of silver citrate complex in nanoscale confinement: An unusual mechanism of formation and growth of silver nanoparticles.," *Langmuir* ., vol. 30, pp. 2460–2469. 2014.

[63] S. K. S. A. G. S. Patra A. K. Pandey, "Wonderful nanoconfinement effect on redox reaction equilibrium.," *RSC Advances.*, vol. 4, pp. 33 366–33369. 2014.

[64] S.-W. O. B.-G. J. C. W. L. J. K. L. H. J. Jang H. Yun, "Asymmetric growth of silver citrate compounds by mechanical stirring and their enhanced antimicrobial activity.," *Bulletin of the Korean Chemical Society.*, vol. 38, pp. 1069–1074. 2017.

[65] S. K. R. Chadha N. Maiti, "Reduction and aggregation of silver ions in aqueous citrate solutions.," *Materials Science and Engineering C.*, vol. 38, pp. 192–196. 2014.

[66] A. A. K. J. B. Deshpande, "Reaction engineering for continuous production of silver nanoparticles.," *Chemical Engineering Technology.*, vol. 41, pp. 157–167. 2018.

[67] H. H. I. P. P. A. G. H. du Toit T. J. Macdonald, "Continuous flow synthesis of citrate capped gold nanoparticles using uv induced nucleation.," *RSC Advances.*, vol. 7, pp. 9632–9638. 2017.

[68] J. M. C. I. Ojea-Jiménez, "Molecular modeling of the reduction mechanism in the citrate-mediated synthesis of gold nanoparticles.," *Journal of Physical Chemistry C* ., vol. 116, pp. 23 682–23691. 2012.

[69] D. I. A. I. G. A. T. M. P. C. M. A. D. E. M. G. C. I. Călinescu D. Martin, "Nanoparticles synthesis by electron beam radiolysis.," *Central European Journal of Chemistry* ., vol. 12, pp. 774–781. 2014.

[70] J. H. P. H. W. K. Y. H. K. H. B. B. C. M. P. B. C. L. H. S. Kang B. Kim, "Size control technology of silver nanoparticles using electron beam irradiation .," *Bulletin of the Korean Chemical Society.*, vol. 34, pp. 3899–3902. 2013.

[71] B. M. W. A. A. T. M. D. A. B. W. Jacobs R. J. T. Houk, "Electron beam synthesis of metal and semiconductor nanoparticles using metal-organic frameworks as ordered precursors.," *Nanotechnology* ., vol. 22, p. 375601. 2011.

[72] Z. Z. G. A. F. R. H. Li Y. Zhao, "Electron-beam induced in situ growth of self-supported metal nanoparticles in ion-containing polydopamine.," *Materials Letters* ., vol. 252, pp. 277–281. 2019.

ACKNOWLEDGEMENTS

First and foremost, I would like extend my gratitude to my supervisor prof. Jong-KuK Lim, for giving me chance to research and providing inestimable guidance and sustain me for over my master process. He inspired me with his perseverance, vision, and integrity. and then I would also like express to my parents for them sufficient support and understanding. last but not the least，I thank all of my friends and labmates for leave me a good memory during my master study.